

Non-Markovian entanglement transfer to distant atoms in a coupled superconducting resonator

Qingxia Mu(穆青霞), Peiying Lin(林佩英)

Citation: Chin. Phys. B . 2020, 29(6): 060304 . **doi:** 10.1088/1674-1056/ab84d8
Journal homepage: http://cpb.iphy.ac.cn; http://iopscience.iop.org/cpb

What follows is a list of articles you may be interested in

Generating Kerr nonlinearity with an engineered non-Markovian environment

Fei-Lei Xiong(熊飞雷), Wan-Li Yang(杨万里), Mang Feng(冯芒)

Chin. Phys. B . 2020, 29(4): 040302 . **doi:** 10.1088/1674-1056/ab7741

Dipole-dipole interactions enhance non-Markovianity and protect information against dissipation

Munsif Jan, Xiao-Ye Xu(许小冶), Qin-Qin Wang(王琴琴), Zhe Chen(陈哲), Yong-Jian Han(韩永建), Chuan-Feng Li(李传锋), Guang-Can Guo(郭光灿)

Chin. Phys. B . 2019, 28(9): 090303 . **doi:** 10.1088/1674-1056/ab37f2

Dynamics of two levitated nanospheres nonlinearly coupling with non-Markovian environment

Xun Li(李逊), Biao Xiong(熊标), Shilei Chao(晁石磊), Jiasen Jin(金家森), Ling Zhou(周玲)

Chin. Phys. B . 2019, 28(5): 050302 . **doi:** 10.1088/1674-1056/28/5/050302

Quantifying quantum non-Markovianity via max-relative entropy

Yu Luo(罗宇), Yongming Li(李永明)

Chin. Phys. B . 2019, 28(4): 040301 . **doi:** 10.1088/1674-1056/28/4/040301

Optomechanical state transfer between two distant membranes in the presence of non-Markovian environments

Jiong Cheng(程泂), Xian-Ting Liang(梁先庭), Wen-Zhao Zhang(张闻钊), Xiangmei Duan(段香梅)

Chin. Phys. B . 2018, 27(12): 120302 . **doi:** 10.1088/1674-1056/27/12/120302

Non-Markovian entanglement transfer to distant atoms in a coupled superconducting resonator*

Qingxia Mu(穆青霞)† and Peiying Lin(林佩英)

Mathematics and Physics Department, North China Electric Power University, Beijing 102206, *China*

(Received 12 February 2020; revised manuscript received 11 March 2020; accepted manuscript online 31 March 2020)

We investigate the non-Markovian effects on the entanglement transfer to the distant non-interacting atom qubits, which are embedded in a coupled superconducting resonator. The master equation governing the dynamics of the system is derived by the non-Markovian quantum state diffusion (NMQSD) method. Based on the solution, we show that the memory effect of the environment can lead to higher entanglement revival and make the entanglement last for a longer time. That is to say, the non-Markovian environment can enhance the entanglement transfer. It is also found that the maximum entanglement transferred to distant atoms can be modified by appropriately selecting the frequency of the modulated inter-cavity coupling. Moreover, with the initial anti-correlated state, the entanglement between the cavity fields can be almost completely transferred to the separated atoms. Lastly, we show that the memory effect has a significant impact on the generation of entanglement from the initial non-entangled states.

Keywords: non-Markovian, entanglement transfer, quantum state diffusion

PACS: 03.67.Pp, 03.65.Yz **DOI:** 10.1088/1674-1056/ab84d8

1. Introduction

The non-classical property of quantum entanglement is one of the most important characteristics of quantum physics. It is beneficial to understanding of the basic theory of quantum mechanics and has potential applications in quantum information processing and quantum communication.[1] Faithful transfer of quantum state between two distant sites is an essential task in quantum technology, which can be realized either by teleportation or quantum networking.[2–5] In the past, cavity quantum electrodynamics (QED) that can be applied to study the interaction between atoms and quantized electrodynamics has been shown to be a promising and natural framework for the further study of entanglement control and manipulation.[6–11] The implementation of cavity QED architecture can be extended to the superconducting circuit systems, constructed by Josephson junctions and various electronic components, which is usually called circuit QED.[12] Generally, the superconducting qubit is often referred to as an artificial atom that can be designed for various research purposes. Hence, the solid-state superconducting circuits have been proved to be an efficient tool to realize quantum information processing, such as the implementation of entangled states,[13,14] quantum state transfer,[15,16] and quantum logic gates.[17]

However, the difficulties arise, e.g., any realistic quantum system will inevitably interact with its surroundings and thus leads to quantum disentanglement or limits the fidelity of quantum state transfer.[18] Many efforts have been devoted to finding approaches for entanglement protection in quantum open systems, such as quantum error correction,[19–21] quantum Zeno effect,[22] and dynamical decoupling.[23] Conventionally, when the system and environment are weakly coupled, the environment with short memory time can be regarded as Markovian dynamics. However, in many cases, the weak-coupling approximation is not applicable, thus the memory effect cannot be neglected, which corresponds to non-Markov process.[24–27] The effect of non-Markov process on decoherence and disentanglement of an open system is obviously different from the Markov process due to the back flow of information.[28,29] It has been shown that engineering structured non-Markovian environment is also meaningful to protect the system from the decoherence.[30–33]

In this paper, we focus on the influence of the memory effect on the entanglement transfer to the distant artificial atoms in non-Markovian reservoirs, from the master equation of the system derived by the NMQSD approach.[28,34–39] It is a newly developed technique in both analytical treatments and numerical simulations to solve non-Markovian dynamics of quantum open systems. Our results show that the environmental memory can lead to long-lasting and higher revived entanglement, thus the non-Markovian properties play a major role in the entanglement transfer and generation. Also, the impact of the modulated inter-cavity coupling on the entanglement transfer is studied.

The paper is organized as follows. In Section 2, we introduce the system and derive the master equation using the NMQSD approach. In Section 3, we analyze in detail the influ-

*Project supported by the Fundamental Research Funds for the Central Universities, China (Grant No. 2018MS056) and the National Natural Science Foundation of China (Grant Nos. 11605055 and 11974108).

†Corresponding author. E-mail: qingxiamu@ncepu.edu.cn

© 2020 Chinese Physical Society and IOP Publishing Ltd

ence of non-Markovian environment on entanglement transfer and entanglement generation in the rotating wave approximation. In addition, we also examine the relationship between the modulated inter-cavity coupling and the entanglement transfer. Finally we draw conclusions in Section 4.

2. Model and solution

The model we consider is composed of two coupled cavities, each of them also interacts with independent single qubit. The possible setup for the implementation of the scheme can be realized in a circuit QED system, as shown in Fig. 1, where the cavities are effectively represented by LC circuits. The coupling between two cavities is implemented through a superconducting quantum interference device (SQUID). Each cavity is coupled to a superconducting transmon qubit, which is composed of two Josephson junctions and called a two-level artificial atom. The total Hamiltonian of this system plus a non-Markovian environment can be written as (setting $\hbar = 1$)

$$H_{\rm tot} = H_{\rm S} + H_{\rm B} + H_{\rm int}, \tag{1}$$

with

$$\begin{aligned} H_{\rm S} =& \sum_{k=1}^{2} \left[\omega_k a_k^\dagger a_k + \frac{\omega_{a_k}}{2}\sigma_k^z + \lambda_k(\sigma_k^+ a_k + \sigma_k^- a_k^\dagger) \right] \\ &+ \alpha(t)(a_1^\dagger + a_1)(a_2^\dagger + a_2) \end{aligned} \tag{2}$$

being the Hamiltonian of the system composed of the cavities and artificial atoms, which can be described by the Jaynes–Cummings-type interactions. Here a_k and $a_k^\dagger$ are the annihilation and creation operators of the cavity modes with eigenfrequencies ω_k, and σ_k^+ and σ_k^- are the rise and fall operators of the atoms with transition frequencies ω_{a_k}, respectively. The parameter λ_k is the coupling coefficient between the atom and the corresponding cavity field; $\alpha(t) = \alpha_0 \cos(\Omega t)$ indicates the time-dependent coupling strength between two resonator modes with α_0 and Ω being the modulation amplitude and frequency, respectively. The time-dependent coupling can be realized by modulating the inductance of the SQUID, which will change the boundary condition of the cavities and their interaction.[40,41]

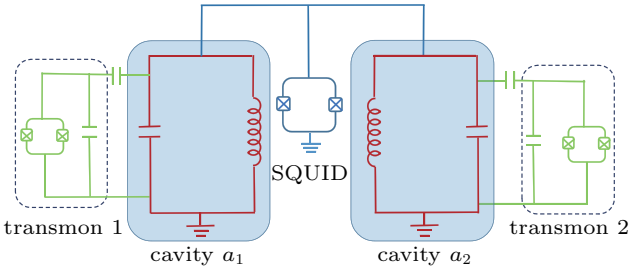


Fig. 1. Schematic of a circuit-QED design for our scheme. Two cavities interact via a SQUID-mediated tunable coupler, and each resonator mode is coupled to a superconducting transmon qubit.

We assume that the system is coupled to a bosonic bath which can be described by

$$H_{\rm B} = \sum_j \nu_j b_j^\dagger b_j, \tag{3}$$

where b_j and $b_j^\dagger$ are annihilation and creation operators satisfying $[b_j b_{j'}^\dagger] = \delta_{j,j'}$. The interaction between the system and the environment is expressed as

$$H_{\rm int} = \sum_j g_j b_j^\dagger L + {\rm H.c.}, \tag{4}$$

where g_j is the system-bath coupling strength, and $L = a_1 + a_2$ is the system Lindblad operator coupled to the environment. Here we assume that the major dissipative channel is from the leakage of the two cavities, and the spontaneous emission of the atom is omitted. This assumption is reasonable under certain conditions since the lifetime of the qubits is much longer than that of cavities due to the relatively weak coupling with the environment.[42] Here we focus exclusively on the vacuum environment.

In the following we solve the model using the NMQSD approach. It can be proved that the full wavefunction of the total system including both the state of system and environment can be represented by a stochastic pure state called the quantum trajectory as follows:

$$\begin{aligned} &\frac{\rm d}{{\rm d}t}|\Psi(t,z^*)\rangle \\ &= \left[-{\rm i}H_{\rm S} + Lz^* - L^\dagger \int {\rm d}s \alpha(t,s) \frac{\delta}{\delta z_s^*} \right] |\Psi(t,z^*)\rangle, \end{aligned} \tag{5}$$

with $z_t^* = -{\rm i}\sum_j g_j z_j^* {\rm e}^{{\rm i}\nu_j t}$ being the complex Gaussian variable satisfying $M[z_t] = M[z_t z_s] = 0$ and $M[z_t^* z_s] = \alpha(t,s)$, and $M[\cdot] \equiv \int \frac{{\rm d}z^2}{\pi} {\rm e}^{-|z|^2}[\cdot]$ stands for the statistical average over the noise z_t. For the zero-temperature environment, the bath correlation function of the noise is $\alpha(t,s) = \sum_j |g_j|^2 {\rm e}^{-{\rm i}\nu_j(t-s)}$. However, the non-Markovian QSD Eq. (5) is difficult to be implemented as an analytical or numerical tool due to the existence of the time-nonlocal term. In order to solve the above equation, we introduce a time-dependent operator O to replace the functional derivative as $\frac{\delta}{\delta z_s^*}|\Psi(t,z^*)\rangle \equiv O(t,s,z^*)|\Psi(t,z^*)\rangle$. Then the NMQSD equation can be transformed to

$$\frac{\rm d}{{\rm d}t}|\Psi(t,z^*)\rangle = \left[-{\rm i}H_{\rm S} + Lz^* - L^\dagger \bar{O}(t,z^*) \right] |\Psi(t,z^*)\rangle, \tag{6}$$

where $\bar{O}(t,z^*) \equiv \int_0^t {\rm d}s \alpha(t,s) O(t,s,z^*)$ under the initial condition $O(t,s=t,z^*) = L$. Notably, the non-Markovian properties are mainly encoded in the operator O, and hence in a finite width correlation function $\alpha(t,s)$. Hereafter, we consider the Ornstein–Uhlenbeck type correlation function with $\alpha(t,s) = \frac{\Gamma\gamma}{2} {\rm e}^{-\gamma|t-s|}$, where Γ is the global decay rate, and $1/\gamma$ represents the memory time of the environment. When γ approaches to zero, it will manifest a strong non-Markovian

effect. As a comparison, when $\gamma\to\infty$, $\alpha(t,s)$ can be approximately reduced to the Dirac delta function, which corresponds to the Markov limit. Equation (6) is then simplified to the standard Markovian QSD equation.[43] Therefore, in the QSD approach, it is crucially important to determine the form of O operator so as to obtain the complete non-Markovian information.

Actually, using the consistency condition

$$\frac{\partial}{\partial t}\frac{\delta}{\delta z_s^*}|\Psi(t,z^*)\rangle=\frac{\delta}{\delta z^*}\frac{\partial}{\partial t}|\Psi(t,z^*)\rangle,$$

the evolution of O operator is given as

$$\frac{\partial}{\partial t}O=\left[-\mathrm{i}H_s+Lz_t^*-L^\dagger\bar{O},O\right]-L^\dagger\frac{\delta}{\delta z_s^*}\bar{O}.$$

Then it is clear that the O operator for this particular model can be expanded as

$$\begin{aligned}O(t,s) &= f_1(t,s)a_1+f_2(t,s)a_2+f_3(t,s)a_1^\dagger\\ &\quad+f_4(t,s)a_2^\dagger+f_5(t,s)\sigma_1^-+f_6(t,s)\sigma_2^-,\end{aligned}\tag{7}$$

where the time-dependent coefficients $f_i(t,s)$ satisfy

$$\frac{\partial}{\partial t}f_1 = \mathrm{i}\omega_1 f_1a_1+\mathrm{i}\alpha(t)f_2-\mathrm{i}\alpha(t)f_4+F_1f_1+F_1f_2,\tag{8}$$

$$\frac{\partial}{\partial t}f_2 = \mathrm{i}\omega_2 f_2+\mathrm{i}\alpha(t)f_1-\mathrm{i}\alpha(t)f_3+F_2f_1+F_2f_2,\tag{9}$$

$$\begin{aligned}\frac{\partial}{\partial t}f_3 &= -\mathrm{i}\omega_1 f_3+\mathrm{i}\alpha(t)f_2-\mathrm{i}\alpha(t)f_4+2F_3f_1\\ &\quad+F_4f_2-F_1f_3-F_2f_4+F_3f_2,\end{aligned}\tag{10}$$

$$\begin{aligned}\frac{\partial}{\partial t}f_4 &= -\mathrm{i}\omega_1 f_4+\mathrm{i}\alpha(t)f_1-\mathrm{i}\alpha(t)f_3\\ &\quad+F_4f_1+F_4f_2+F_3f_1-F_1f_3-F_2f_4,\end{aligned}\tag{11}$$

$$\frac{\partial}{\partial t}f_5 = \mathrm{i}\lambda_1 f_1+\mathrm{i}\omega_{a1}f_5+F_5f_1+F_5f_2,\tag{12}$$

$$\frac{\partial}{\partial t}f_6 = \mathrm{i}\lambda_2 f_2+\mathrm{i}\omega_{a2}f_6+F_6f_1+F_6f_2,\tag{13}$$

with $F_i(t)=\int_0^t\alpha(t,s)f_i(t,s)\,\mathrm{d}s$ $(i=1,\ldots,6)$ under the boundary conditions

$$f_i(t=s,s)=1\quad(i=1,2),\tag{14}$$

$$f_j(t=s,s)=0\quad(j=3,4,5,6).\tag{15}$$

With the determined coefficient functions, the reduced density matrix of the system can be recovered by taking the statistical mean of all the generated trajectories,

$$\rho_t=M\left[|\Psi_t(z^*)\rangle\langle\Psi_t(z^*)|\right].\tag{16}$$

Furthermore, we can also derive the mast equation based on Eq. (6) as follows:

$$\begin{aligned}\frac{\mathrm{d}}{\mathrm{d}t}\rho &= -\mathrm{i}[H_\mathrm{S},\rho]+\{[L,\rho\bar{O}^\dagger]+\mathrm{H.c.}\}\\ &= -\mathrm{i}\sum_{l=k}^{2}\left[\omega_k a_k^\dagger a_k+\frac{\omega_{\mathrm{ak}}}{2}\sigma_k^z+\lambda_k\left(\sigma_k^+a_k+\sigma_k^-a_k^\dagger\right),\rho\right]\\ &\quad-\mathrm{i}\left[\alpha(t)\left(a_1^\dagger+a_1\right)\left(a_2^\dagger+a_2\right),\rho\right]\\ &\quad+\left\{F_1^*\sum_{k=1}^{2}\left(a_k\rho a_1^\dagger-\rho a_1^\dagger a_k\right)\right.\\ &\quad+F_2^*\sum_{k=1}^{2}\left(a_k\rho a_2^\dagger-\rho a_2^\dagger a_k\right)\\ &\quad+F_3^*\sum_{k=1}^{2}\left(a_k\rho a_1-\rho a_1a_k\right)+F_4^*\sum_{k=1}^{2}\left(a_k\rho a_2-\rho a_2a_k\right)\\ &\quad+F_5^*\sum_{k=1}^{2}\left(a_k\rho\sigma_1^\dagger-\rho\sigma_1^\dagger a_k\right)\\ &\quad\left.+F_6^*\sum_{k=1}^{2}\left(a_k\rho\sigma_2^\dagger-\rho\sigma_2^\dagger a_k\right)+\mathrm{H.c.}\right\}.\end{aligned}\tag{17}$$

3. Numerical results and discussion

Having developed the time-local non-Markovian QSD equation for the system, we now concern about the entanglement generation and entanglement transfer from the cavity modes to the atom qubits. Throughout this paper, we employ the well-known concurrence measure defined by Wootters to quantify the degree of entanglement for any two-qubit system, which can be expressed as[44]

$$C(t)=\max\{0,\sqrt{\lambda_1}-\sqrt{\lambda_2}-\sqrt{\lambda_3}-\sqrt{\lambda_4}\},\tag{18}$$

where the quantities λ_i are the eigenvalues in the decreasing order of the matrix

$$\rho_{\mathrm{AB}}(\sigma_y^{(1)}\otimes\sigma_y^{(2)})\rho_{\mathrm{AB}}^*(\sigma_y^{(1)}\otimes\sigma_y^{(2)}),\tag{19}$$

and ρ_{AB} is the density operator of the bipartite system.

In Eq. (2), the coupling between two cavities is written in its full form which contains the counter-rotating terms $a_1^\dagger a_2^\dagger$ and a_1a_2. In this subsection, we mainly study the the entanglement transfer from the cavity fields to the qubits under the rotating-wave approximation, which is a widely used approximation to keep only energy-conserving terms in the Hamiltonian.[45] Under the conditions $|\omega_1-\omega_2|\ll\omega_1+\omega_2$ and $\omega_1+\omega_2\gg\alpha_0$, the rotating-wave approximation is valid so that the counter-rotating terms can be neglected, and then the coefficients f_3 and f_4 of the O operator reduce to zero.

We are now able to investigate the state transfer performance from cavities to the separated atom qubits. We assume that there is at most one excitation in the system since we are interested in the dynamics of entanglement transfer at zero temperature. Initially we have non-entangled atom qubits and entangled photons. For instance, we choose the two cavity modes prepared in one of their Bell states $|\phi^+\rangle=\frac{1}{\sqrt{2}}(|10\rangle+|01\rangle)$ and both the two atoms prepared in ground states $|gg\rangle$. We numerically simulate the evolution from the initial states, and the entanglement transferred from the cavities to the atoms can be measured by concurrence since there are no more than one photon excited under the rotating-wave

approximation. The time evolution of the entanglement between the two atoms and the two cavities is plotted in Fig. 2. The numerical results show that the concurrences swap back and forth between the atoms and cavities in a repeatable fashion, and both of them exhibit oscillations similar to a sine-cosine envelope. This means that the entanglement is periodically transferred to the atoms though the amounts of concurrences are decreasing due to the interaction with the environment. Next, we will focus on how the external environment affects the entanglement transfer.

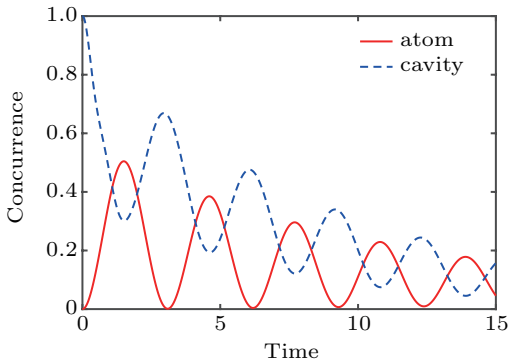


Fig. 2. The time evolution of the entanglement transfer. The initial state is prepared in $\frac{1}{\sqrt{2}}(|10\rangle+|01\rangle)\otimes|gg\rangle$. The other parameters are $\omega_1=\omega_2=5$, $\omega_{a1}=\omega_{a2}=5$, $\lambda_1=\lambda_2=0.8$, $\alpha_0=1$, $\gamma=2$, $\Omega=0$, $\Gamma=1$.

In order to analyze the influence from the non-Markovian environment on the entanglement transfer, we plot the time evolution of the two-atom entanglement for different memory times indicated by $1/\gamma$, as shown in Fig. 3(a). Here the initial state of the system is still prepared in $\Psi_{\rm ini}=\frac{1}{\sqrt{2}}(|10\rangle+|01\rangle)\otimes|gg\rangle$. We observe that when the memory time is longer (γ is smaller), which corresponds to the non-Markovian environment, there will be entanglement revivals after the entanglement suffers a sudden death. However, in the case of short memory time (γ is larger), which means the transition of the environment from non-Markovian to the Markovian regions, the revival of the concurrence is restrained. Therefore, long-lasting and higher revived two-qubit entanglement can be observed in the non-Markovian environment due to the back reaction or information backflow. Moreover, the maximum entanglement that can be transferred to the atoms is also studied. Figure 3(b) shows the maximum concurrence of the atoms as a function of γ. It is obvious that the maximum value of entanglement transferred to the atoms achieves a higher value for a longer memory time (smaller γ). In summary, the results in Fig. 3 imply that the non-Markovian memory effect is of great benefit to the entanglement transfer into the atoms.

Apart from the memory time, some other parameters of the system also play an important role in the entanglement dynamics. Therefore, in order to achieve higher entanglement transfer, it is truly important to tune the parameters to certain optimal values in the actual experiment. In the following, we investigate the influence of some parameters such as the modulated inter-cavity amplitude and frequency on the entanglement transfer. In Fig. 4, we plot the time evolution of the two-atom entanglement for different inter-cavity coupling frequencies Ω. As shown in Fig. 4(a), the entanglement increases first and then attains its higher value in the appropriate range of Ω. The maximum entanglement transfer $\max\{C\}$ is explicitly plotted in Fig. 4(b), where $\max\{C\}$ increases with Ω. Therefore, the dynamics of the qubit entanglement can be modified by choosing the time dependent coupling between cavity fields. The modulated inter-cavity coupling can provide entanglement protection.

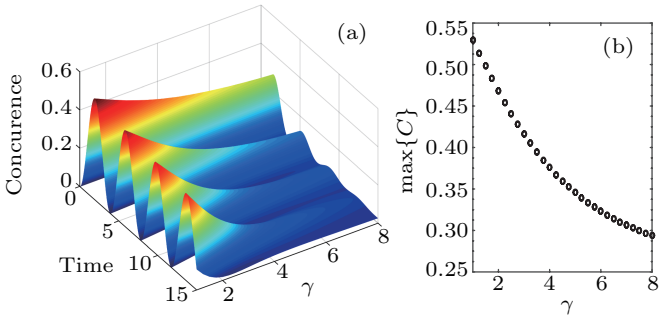


Fig. 3. Non-Markovian impact on entanglement transferred to atoms: (a) the dynamics of two-atom entanglement for different values of γ, (b) the maximum coherence transfer that can be achieved. The initial state is prepared in $\frac{1}{\sqrt{2}}(|10\rangle+|01\rangle)\otimes|gg\rangle$. The other parameters are $\omega_1=\omega_2=5$, $\omega_{a1}=\omega_{a2}=5$, $\lambda_1=\lambda_2=0.6$, $\alpha_0=1$, $\Omega=0$, $\Gamma=0.5$.

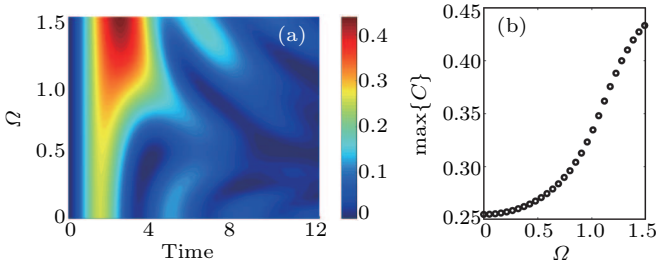


Fig. 4. Two-atom entanglement for different inter-cavity coupling frequencies Ω. The initial state is prepared in $\frac{1}{\sqrt{2}}(|10\rangle+|01\rangle)\otimes|gg\rangle$. The other parameters are $\omega_1=\omega_2=5$, $\omega_{a1}=\omega_{a2}=5$, $\lambda_1=\lambda_2=0.6$, $\alpha_0=1$, $\gamma=4$, $\Gamma=1$.

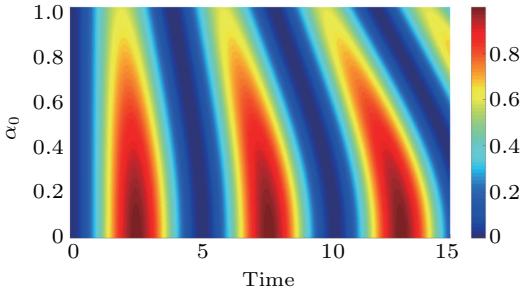


Fig. 5. Two-atom entanglement for different inter-cavity coupling amplitudes α_0. The initial state is prepared in $\frac{1}{\sqrt{2}}(|10\rangle-|01\rangle)\otimes|gg\rangle$. The other parameters are $\omega_1=\omega_2=5$, $\omega_{a1}=\omega_{a2}=5$, $\lambda_1=\lambda_2=0.6$, $\gamma=2$, $\Omega=0$, $\Gamma=1$.

In Fig. 5, we plot the time evolution of the two-atom entanglement with different inter-cavity coupling parameters α_0. Here we simulate the dynamics starting with the anti-correlated state $\Psi_{\rm ini}=\frac{1}{\sqrt{2}}(|10\rangle-|01\rangle)\otimes|gg\rangle$. As shown in

Fig. 5, the advantage of this initial state is that the entanglement between the cavity fields can be almost completely transferred to the separated atoms. It is obvious that with the increase of the coupling parameter α_0, the entanglement of atoms decreases but the transfer speed increases. This is because the anti-correlated states are in the decoherence free space of the Hamiltonian for cavities, so that it suffers less decoherence in the transfer process. The results show that the coupling parameters between the two cavity fields play an important role in the entanglement transfer.

Finally, we consider the performance of the entanglement generation. Initially we have both non-entangled atoms and non-entangled photons. Figures 6(a) and 6(c) show the dynamics of entanglement generation from the initial states of $|e,g,0,0\rangle$ and $|g,g,1,0\rangle$, respectively. The red solid line reveals the concurrence of two atoms, while the blue dashed line represents the concurrence between cavity fields. It is clear that both unentangled photons and atoms quickly get entangled. The corresponding maximum entanglement with different memory times is plotted in Figs. 6(b) and 6(d). It is revealed that when the environment is closer to non-Markov (smaller γ), the maximum entanglement value is larger. On the contrary, the closer the environment is to Markov (larger γ), the smaller the maximum entanglement value is. Therefore, the properties of the environment have a significant impact on the generation of entanglement.

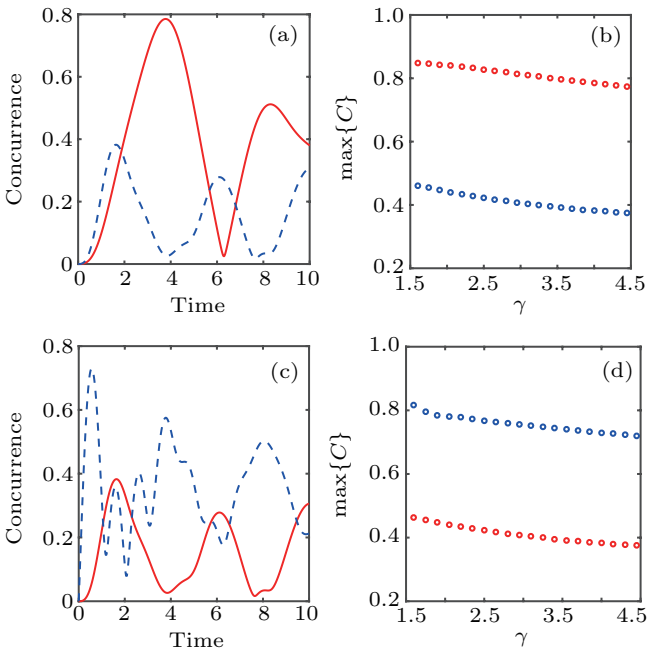


Fig. 6. Dynamics of entanglement generation: (a) and (c) the evolution of the concurrence for different initial states $|e,g,0,0\rangle$ and $|g,g,1,0\rangle$, respectively; (b) and (d) the corresponding maximum entanglement $\max\{C\}$ for different γ. The red solid curve represents the entanglement between atoms, and the blue dashed curve is the entanglement between the cavity fields. For (a) and (c), $\gamma = 4$. The other parameters are chosen as $\omega_1 = \omega_2 = 5$, $\omega_{a1} = \omega_{a2} = 5$, $\lambda_1 = \lambda_2 = 0.6$, $\alpha_0 = 1$, $\Omega = 0, \Gamma = 1$.

4. Discussion and conclusion

In summary, we have studied the dynamics of the entanglement transfer to the distant atom qubits, which are embedded in two separated lossy cavities connected by SQUID-mediated tunable coupler. Actually, the cavities are coupled to a non-Markovian environment instead of a Markovian one. A general master equation for the concerned system can be obtained by the NMQSD approach. We first analyze the influence of the memory effect on the entanglement transfer under the rotating-wave approximation. It is found that the longer memory time is helpful for entanglement transfer, and the non-Markovian effect will lead to a stronger entanglement revival phenomenon. Another major procedure is that the coupling between two resonator modes is time-dependent, which can be realized by modulating the inductance of the SQUID. Also, it helps to optimize the maximum entanglement transferred to the atoms by appropriately selecting the frequency of the inter-cavity coupling. In addition, we show that the entanglement of the resonator modes with the initial anti-correlated state can be almost completely transferred to the atoms. Finally we investigate the non-Markovian effects on the entanglement generation with initial separated sates.

References

[1] Jones J A and Jaksch D 2012 *Quantum Information, Computation and Communication* (Cambridge: Cambridge University Press)
[2] Pirandola S, Eisert J, Weedbrook C, Furusawa A and Braunstein S L 2015 *Nat. Photon.* **9** 641
[3] Cleve R and Buhrman H 1997 *Phys. Rev. A* **56** 1201
[4] Chen Z H, Zhang F Y, Shi Ying and Song H S 2012 *Chin. Phys. Lett.* **29** 090304
[5] Yang G, Lian B W, Nie M and Jin J 2017 *Chin. Phys. B* **26** 040305
[6] Kim M S and Agarwal G S 1999 *Phys. Rev. A* **59** 3044
[7] Solano E, Agarwal G S and Walther H 2003 *Phys. Rev. Lett.* **90** 027903
[8] Mu Q X, Ma Y H and Zhou L 2010 *Phys. Rev. A* **81** 024301
[9] Akram U, Bowen W P and Milburn G J 2013 *New J. Phys.* **15** 093007
[10] Dehghani A, Mojaveri B, Bahrbeig R J, Nosrati F and Franco R L 2019 *J. Opt. Soc. Am. B* **36** 1858
[11] Chen Y H, Xia Y, Chen Q Q and Song J 2015 *Phys. Rev. A* **91** 012325
[12] Gu X, Kockum A F, Miranowicz A, Liu Y X and Nori F 2017 *Phys. Rep.* **718–719** 1
[13] Wang C, Gao Y Y, Reinhold P, Heeres R W, Ofek N, Chou K, Axline C, REagor M, Blumoff J, Sliwa K M, Frunzio L, Girvin S M, Jiang L, Mirrahimi M, Devoret M H and Schoelkopf R J 2016 *Science* **352** 1087
[14] Ma S L, Xie J K, Li X K and Li F L 2019 *Phys. Rev. A* **99** 042317
[15] Srinivasan S J, Sundaresan N M, Sadri D, Liu Y, Gambetta J M, Yu T, Girvin S M and Houck A A 2014 *Phys. Rev. A* **89** 033857
[16] Axline C J, Burkhart L D, Pfaff W, Zhang M Z, Chou K, Campagne-lbarcq P, Reinhold P, Frunzio L, Girvin S M, Jiang L, Devoret M H and Schoelkopf 2018 *Nat. Phys.* **14** 705
[17] Rosenblum S, Gao Y Y, Reinhold P, Wang C, Axline C J, Frunzio L, Girvin S M, Jiang L, Mirrahimi M, Devoret M H and Schoelkopf R J 2018 *Nat. Commun.* **9** 652
[18] Caruso F, Giovannetti V, Lupo C and Mancini S 2014 *Rev. Mod. Phys.* **86** 1203
[19] Shor P W 1995 *Phys. Rev. A* **52** R2493
[20] Steane A M 1996 *Phys. Rev. Lett.* **77** 793
[21] Zhao X Y, Hedemann S R and Yu T 2013 *Phys. Rev. A* **88** 022321
[22] Maniscalco S, Francica F, Zaffino R L, Lo Gullo N and Plastina F 2008 *Phys. Rev. Lett.* **100** 090503

[23] De Lange G, Wang Z H, Ristè D, Dobrovitski V V and Hanson R 2010 *Science* **330** 60

[24] Breuer H P, Laine E M, Piilo J and Vacchini B 2016 *Rev. Mod. Phys.* **88** 021002

[25] Laine E M, Piilo J and Breuer H P 2010 *Phys. Rev. A* **81** 062115

[26] Wißmann S, Breuer H P and Vacchini B 2015 *Phys. Rev. A* **92** 042108

[27] Shen H Z, Li D X, Su S L, Zhou Y H and Yi X X 2017 *Phys. Rev. A* **96** 033805

[28] Mu Q X, Zhao X Y and Yu T 2016 *Phys. Rev. A* **94** 012334

[29] Cheng J, Zhang W Z, Zhou L and Zhang W 2016 *Sci. Rep.* **6** 23678

[30] Leggio B, Lo Franco R, Soares-Pinto D O, Horodecki P and Compagno G 2015 *Phys. Rev. A* **92** 032311

[31] Costa-Filho J I, Lima R B B, Paiva R R, M P, Morgado W A M, Lo Franco R and Soares-Pinto D O 2017 *Phys. Rev. A* **95** 052126

[32] De Vega I and Alonso D 2017 *Rev. Mod. Phys.* **89** 015001

[33] Mu Q X, Li H, Huang X and Zhao X Y 2018 *Opt. Commun.* **426** 70

[34] Diósi L, Gisin N and Strunz W T 1998 *Phys. Rev. A* **58** 1699

[35] Strunz W T, Diósi L and Gisin N 1999 *Phys. Rev. Lett.* **82** 1801

[36] Yu T, Diósi L, Gisin N and Strunz W T 1999 *Phys. Rev. A* **60** 91

[37] Zhao X, Jing J, Corn B and Yu T 2011 *Phys. Rev. A* **84** 032101

[38] Chen M and You J Q 2013 *Phys. Rev. A* **87** 052108

[39] Chen Y, You J Q and Yu T 2014 *Phys. Rev. A* **90** 052104

[40] Felicetti S, Sanz M, Lamata L, Romero G, Johansson G, Delsing P and Solano E 2014 *Phys. Rev. Lett.* **113** 093602

[41] Yang Z P, Li Z, Ma S L and Li F L 2017 *Phys. Rev. A* **96** 012327

[42] Xiang Z L, Ashhab S, You J Q and Nori F 2013 *Rev. Mod. Phys.* **85** 623

[43] Dalibard J, Castin Y and Mølmer K 1992 *Phys. Rev. Lett.* **68** 580

[44] Wootters W K 1998 *Phys. Rev. Lett.* **80** 2245

[45] Scully M O and Zubairy M S 1997 *Quantum optics* (Cambridge: Cambridge University Press)